©2026 Romanian Association of Nonconventional Technologies

DEVELOPMENT OF AN INSULATED ELECTROMECHANICAL ARC TEST BENCH FOR POLARITY-DEPENDENT INVESTIGATION OF ELECTRICAL CONTACTS

Andrei-Dan Tomse[1] and Gabriel Remus Chereghi[2]
[1] Department of Electrical Engineering, University of Oradea, 410087 Oradea, Romania
Corresponding author, ORCID No. 0009-0000-6640-0558, anddantomse@yahoo.com
[2] Department of Forestry, University of Oradea, 410059, Oradea, Romania
ORCID No. 0000-0002-0262-0129, grcheregi@yahoo.com

ABSTRACT: A major challenge in evaluating contactor reliability under arc erosion is the inability to observe contact surfaces during testing, as inspection typically requires disassembly of the device. To address this limitation, an insulated electromechanical arc test bench was developed to study polarity-dependent erosion in Cu–Al contacts under controlled DC switching conditions. The system uses dual-solenoid actuation to ensure stable vertical motion and repeatable arc initiation, while 3D-printed polymer components provide electrical insulation and confine the arc to the contact interface. Repeated switching cycles produced localized melting, shallow crater formation, and surface oxidation at the arc attachment region. Electro-thermal finite element simulations confirmed strong current density constriction and localized Joule heating. These results demonstrate that the proposed platform enables reliable and systematic investigation of arc-induced contact erosion.
KEYWORDS*: arc test bench, electrical contact erosion, polarity-dependent degradation, electro–thermal finite element analysis, additive manufacturing insulation*

1. INTRODUCTION

Electrical contacts are important components used in power distribution systems, switching devices, relays and contactors. When current interruption occurs, the separation of metallic contacts under load produces an electrical arc. The arc plasma can reach localized temperatures between 6,000 and 12,000 K, which leads to melting, vaporization, material transfer and progressive degradation of the contact surface. During repeated switching operations, the morphology of the contacts changes and the electrical resistance gradually increase, which in time can limit the lifetime and reliability of the device. The influence of electrical loading and repeated switching operations on contact resistance has been reported in previous studies [1], while the effects of vibrations and thermally induced disturbances on contact stability have also been investigated in other works [2], [3].

Arc erosion is influenced by several factors such as electrical parameters (current magnitude, voltage level and waveform), mechanical conditions (contact force, separation velocity and contact bounce) and material properties like melting temperature and thermal conductivity. The relationship between contact bounce and the behavior of the electrical arc under resistive and inductive loads has been experimentally studied in the literature [4]. In DC systems, erosion often depends on polarity because the energy deposited at the anode and cathode is not symmetrical. The cathodic region usually presents localized crater formation, while the anodic region tends to show more uniform melting of the material. Experimental investigations regarding arc motion in switching devices also highlight the importance of dynamic arcs in the degradation process of electrical contacts [5]. In AC systems, the periodic reversal of polarity changes the stability of the arc and can produce more symmetrical wear patterns, although restrike and breakdown phenomena can extend the arc duration [6]. Copper-based materials are widely used for electrical contacts because they provide high electrical and thermal conductivity. Composite Cu–Al systems offer advantages related to cost and structural integration, but they can also introduce additional issues such as intermetallic formation, differences in thermal expansion and oxidation when exposed to electrical arcs. Ignition processes that appear due to poor electrical contact conditions further emphasize the need to understand degradation mechanisms in metallic connector systems [7].

To investigate arc erosion under controlled laboratory conditions, a custom electromechanical arc test bench was developed. Previous studies related to striction resistance effects emphasize the need for precise control of both electrical and mechanical parameters during experimental testing [8]. The mechanical structure of the platform and the electrode housing were manufactured using 3D-printed PLA components, which provide electrical insulation and allow a modular configuration of the system.

2. METHODS AND MATERIALS

A custom electromechanical arc erosion test bench was developed to perform controlled make–break operations under electrical load. The structural frame, electrode housings, and guiding components were fabricated using 3D-printed non-conducting PLA polymer material to ensure electrical insulation between conductive elements and the supporting structure.

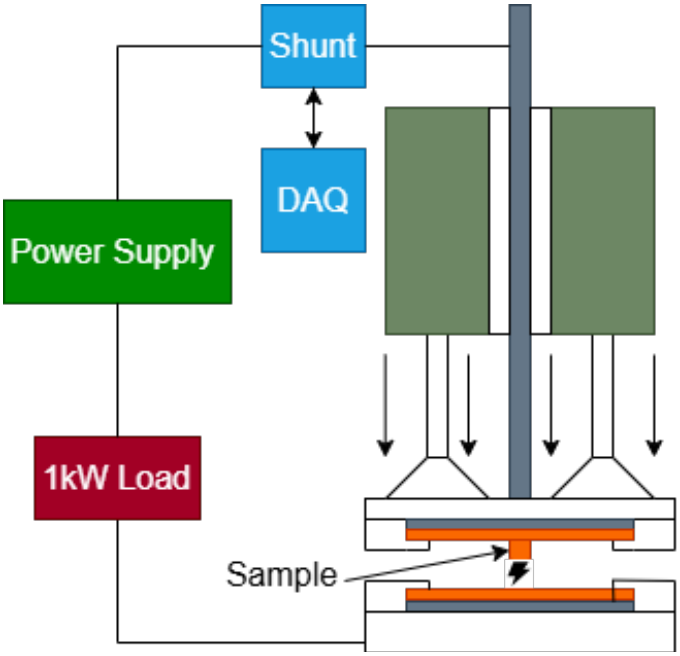

Figure 1. Test Bench diagram

Additive manufacturing enabled precise geometric alignment, modular electrode replacement, and minimization of unintended current paths, by allowing us to test contacts befor and after. All current-carrying components were mechanically isolated from the structural frame, ensuring that arc formation was confined exclusively to the intended contact interface.

The system consists of a vertically aligned electrode pair comprising a moving upper electrode and a fixed lower electrode. The moving electrode assembly was mounted in a guided carriage and actuated using two symmetrically positioned solenoids to ensure uniform vertical displacement and reduced tilting during operation.

A Cu–Al composite sheet containing the desired soldered contact element was installed in the moving holder. The fixed electrode consisted of a polished Cu–Al sheet mounted within a stationary insulated base, which in this test the contact was on the Cu side. Electrical connections were established using low-resistance aluminum conductors to minimize parasitic voltage drop. The polarity of the electrodes was configurable, allowing the moving electrode to operate either as anode or cathode depending on the experimental condition.

Contact motion was achieved using two electromagnetic solenoids mounted parallel to the motion axis. The dual-solenoid configuration provided symmetric constant 10N push-force distribution and improved mechanical stability during contact separation. Separation occurred along a vertical axis to reduce lateral sliding effects and to promote repeatable arc initiation. Actuation timing was controlled using a regulated DC supply with a time relay-contactor setup.

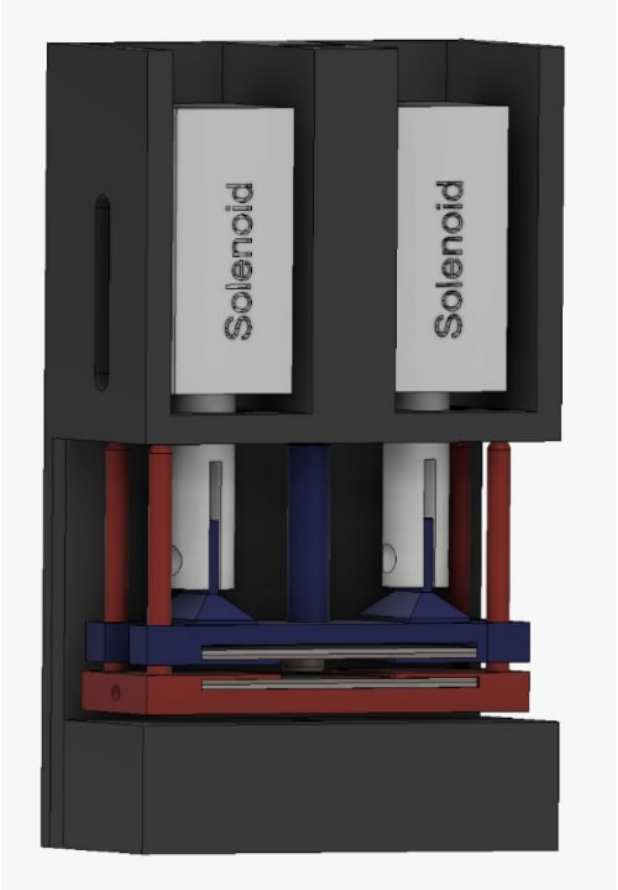

Figure 2. The CAD model of the test bench

Prior to testing, contact surfaces were mechanically polished to obtain a uniform surface finish. The samples were cleaned with isopropyl alcohol to remove contaminants and ensure consistent surface conditions.

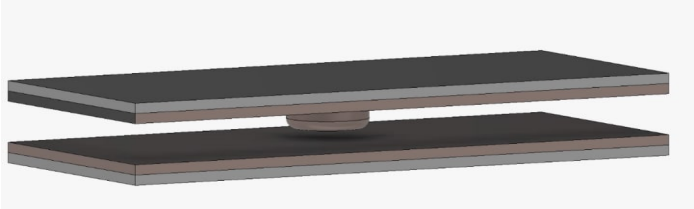

Figure 3. The Contact 3D Model

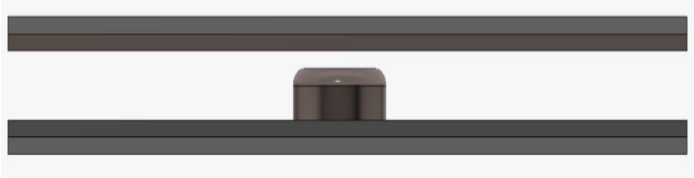

Figure 4. The Contact Profile

The soldered interface between the contact element and the Cu–Al substrate was visually inspected to verify mechanical integrity and electrical continuity.

Arc curent was measured using a calibrated low-resistance shunt resistor connected in series with the test circuit. Arc voltage was measured directly across the electrode terminals using an isolated differential probe and an NI USB 6008 DAQ.

Each test cycle consisted of:

1. Mechanical closure of the contacts
2. Energization of the electrical circuit
3. Controlled separation of the electrodes under load
4. Recording of voltage waveforms
5. Complete arc extinction

Multiple switching cycles were performed under identical electrical and mechanical conditions to evaluate cumulative erosion effects. Separate experimental series were conducted for different polarity configurations to investigate anode–cathode asymmetry.

3. RESULTS

A. Surface Morphology Before and After Arc Exposure

Optical microscopy of the contact prior to arc exposure revealed a relatively uniform metallic surface with consistent reflectivity and fine-scale texture. No visible craters, delamination, or discoloration were observed at the millimeter scale, indicating a homogeneous and undamaged initial condition.

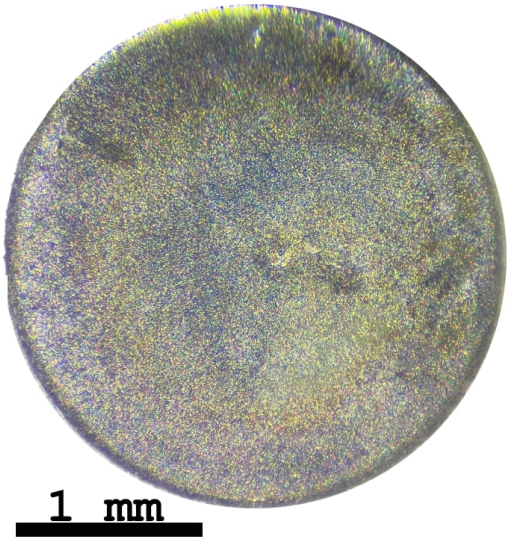

Figure 5. The Contact 3D Model

Following repeated arc switching cycles and subsequent cleaning, significant localized surface modification was observed. Representative micrographs show a heterogeneous morphology concentrated near the geometric center of the contact. The surface exhibits a distinct central modified zone consistent with arc root attachment, surrounded by localized crater-like depressions and irregular solidified melt regions.

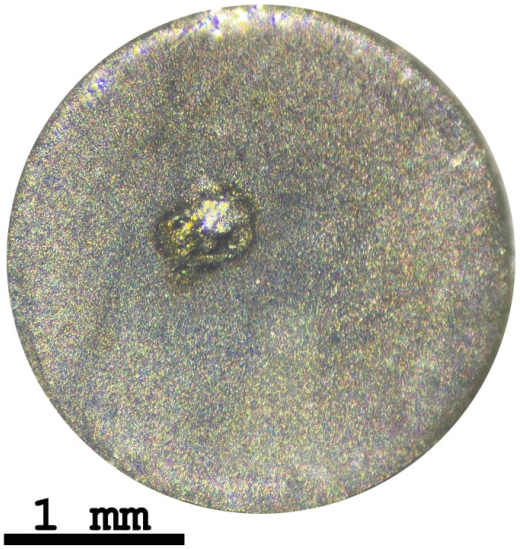

Figure 6. The Contact 3D Model

The central region displays altered reflectivity, indicating localized melting and rapid re-solidification. Based on the 1 mm scale reference, the erosion zone is confined to a region on the order of several hundred micrometers in diameter. Outside this zone, the surface retains much of its original morphology, suggesting that arc energy deposition was spatially concentrated.

Optical microscopy revealed significant surface modification of the Cu–Al contact following repeated arc switching cycles. Representative micrographs of the eroded surface are shown in Fig. 4 and Fig. 5.

B. Melt Pool Formation and Crater Development

The dominant morphological feature is a circular erosion zone centered at the apparent arc attachment site. This region contains shallow crater-like depressions and radially distributed surface modifications. The smooth, reflective appearance of the modified area is consistent with the formation of a transient melt pool followed by rapid quenching as heat dissipated into the bulk material. Surface roughening relative to the peripheral region indicates localized thermal restructuring.

The absence of large, sharply defined cavities suggests that material removal occurred primarily through melting and redistribution rather than explosive ejection. The morphology supports a mechanism dominated by localized melting, molten metal displacement, and re-solidification. Peripheral regions appear less severely affected, confirming that thermal loading was concentrated within the central attachment zone.

C. Surface Oxidation and Thermal Effects

Color variations across the surface are indicative of thin-film interference effects commonly associated with oxide layer formation. These multicolored regions suggest non-uniform thermal exposure during arc sustainment. Differences in coloration between the central and peripheral zones imply variations in peak temperature and cooling rate. The observed features are consistent with high localized temperatures during arc attachment, rapid cooling following arc extinction, and oxidation of exposed metallic surfaces. No persistent carbonaceous deposits were observed after cleaning, indicating that surface modification is primarily thermal and morphological rather than depositional.

D. Material Redistribution

Localized regions with increased reflectivity and irregular surface topology suggest the presence of re-solidified molten material. In several areas, features characteristic of molten metal spreading and micro-scale surface tension driven flow can be observed, together with possible re-deposition of vaporized material. These observations indicate that during arc exposure a temporary melt pool forms on the contact surface, followed by redistribution of the material before solidification occurs.

E. Measured Waveform

The waveform represented in Figure 7, is the voltage measured between two electrical contacts as they separate while current is flowing through the circuit. At the beginning the contacts are closed, so the voltage between them is practically zero because the current flows through direct metal-to-metal conduction.

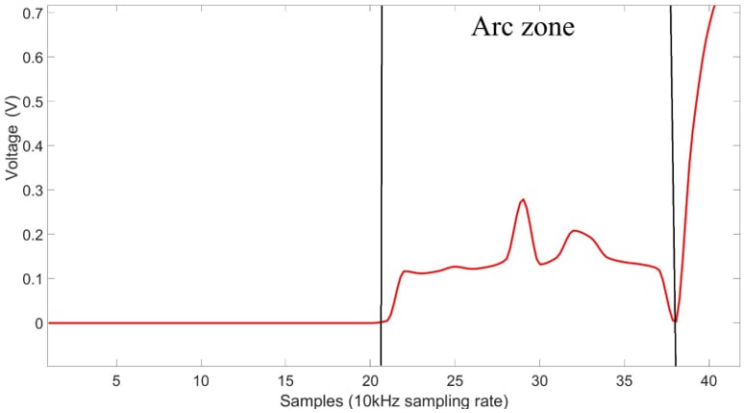

Figure 7. Simulated Total Electric Intensity of the sample

Around sample 20 the contacts start to separate and the metallic bridge breaks, leading to the formation of an electrical arc between the electrodes. The arc acts as a conductive plasma that allows the current to continue flowing across the gap, causing the voltage to rise slightly and fluctuate as the arc length changes and the plasma becomes unstable. As the contacts move further apart, the arc becomes more difficult to sustain and gradually weakens. When the arc finally extinguishes, the conductive plasma channel disappears and the gap becomes insulating. At this moment the open-circuit voltage appears across the contacts, producing the sharp increase observed at the end of the waveform.

4. NUMERICAL SIMULATION RESULTS

Finite element simulations were performed in ANSYS to evaluate the coupled thermal and electrical behavior of the Cu–Al contact during arc attachment. The results include temperature distribution, total electric field intensity, and total current density, as shown in Figures 8–10.

A. Temperature Distribution

The simulated temperature field seen in Figure 8 exhibits a highly localized thermal hotspot centered on the contact surface. The maximum temperature reaches approximately 122.7 °C, while the bulk of the sample remains near the minimum temperature (~20 °C). The isothermal contours are radially symmetric, indicating concentrated heat generation at the arc attachment region and rapid thermal decay toward the periphery. The steep temperature gradient between the central hotspot and surrounding material confirms localized Joule heating. This spatial distribution is consistent with the experimentally observed confined melt crater. Although the simulated peak temperature is lower than actual arc plasma temperatures (which are much higher), it represents the conductive thermal response of the bulk material rather than the plasma column itself. The confinement of elevated temperature to a small region supports the formation of a transient melt pool at the arc root.

B. Electric Field Distribution

The electric field intensity distribution shows a pronounced maximum at the geometric center of the contact, as seen in Figure 9. The peak electric field (~0.086 mV/mm) is concentrated within a small circular region, with radial decay toward the outer boundaries. This localization indicates that current constriction occurs at the arc attachment point. The high electric field gradient drives localized current density enhancement, which in turn increases Joule heating in that region. The symmetric contour pattern suggests stable arc root attachment without significant lateral movement during the simulated condition. The agreement between electric field concentration and the experimentally observed central erosion zone supports the hypothesis that arc stabilization occurred in a confined central region.

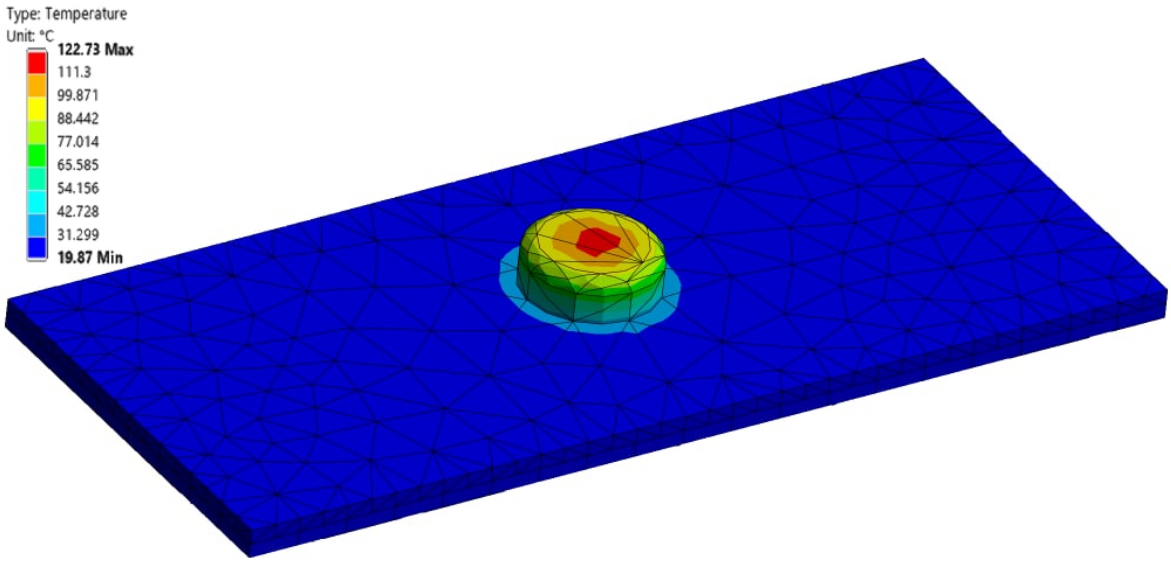

Figure 8. Simulated temperature behaviour of the sample

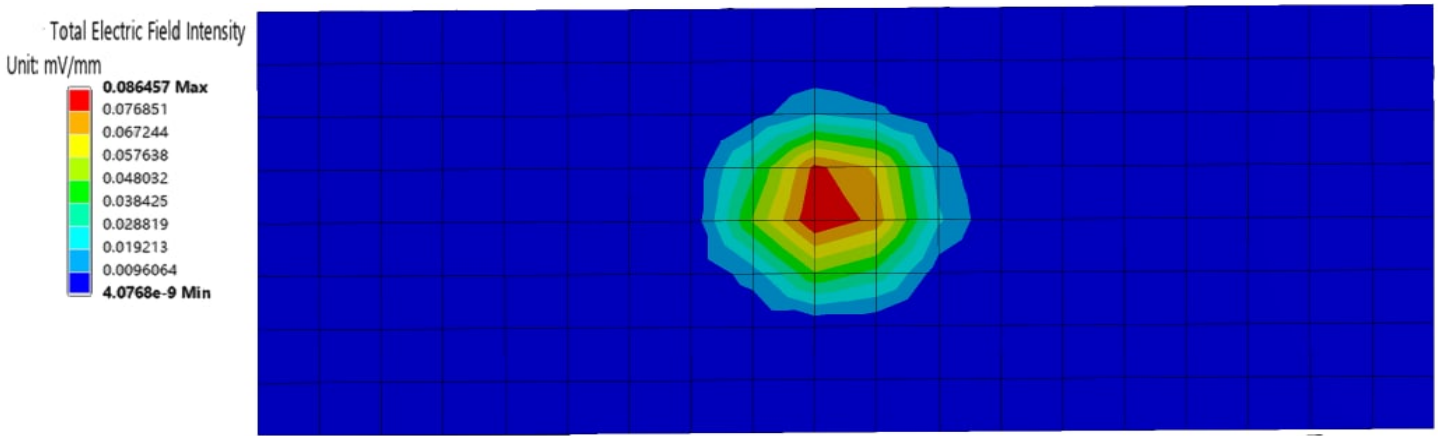

Figure 9. Simulated Total Electric Intensity of the sample

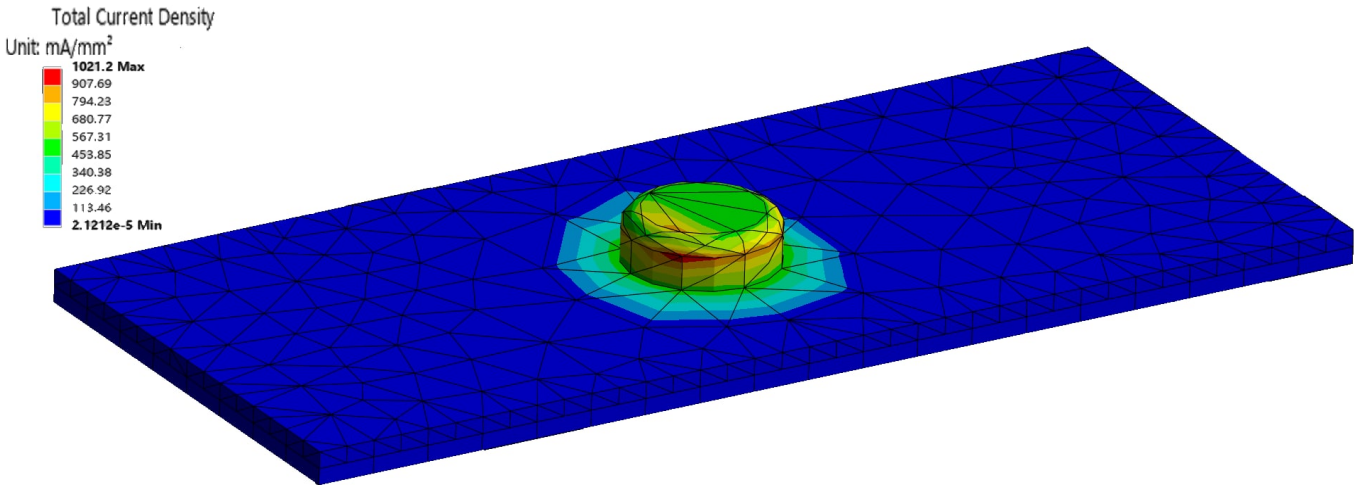

Figure 10. Simulated Total Current Density of the sample

C. Current Density Distribution

The total current density plot reveals strong current crowding at the center of the contact, with a maximum value exceeding 1000 mA/mm². The distribution mirrors the electric field pattern, confirming that electrical loading is highly concentrated at the attachment site.

The steep current density gradient explains the localized thermal damage observed experimentally. Elevated current density leads to increased Joule heating (), producing sufficient thermal energy for localized melting and subsequent re-solidification. The gradual reduction of current density toward the periphery correlates with the limited extent of morphological modification observed in optical microscopy.

The simulation results validate the experimentally observed degradation mechanism: arc-root stabilization produces localized current constriction, generating intense Joule heating that induces melting within a confined central region. The rapid radial decay in temperature and current

density explains the limited spatial extent of surface damage and the absence of widespread structural failure.

5. CONCLUSION

An insulated electromechanical arc test bench was designed and validated for the controlled investigation of polarity-dependent arc erosion in Cu–Al electrical contacts [8], [1]. The structure of the platform was manufactured using 3D-printed polymer components, which ensured electrical insulation between conductive parts and the supporting frame. This configuration confines the current path to the intended contact interface, reducing parasitic conduction and preventing unintended arc formation within the structure [9].

The actuation mechanism based on two symmetrically positioned solenoids provided uniform vertical displacement of the moving electrode and reduced tilting during operation. Because of this configuration, consistent and repeatable make–break operations could be obtained during testing [2]. The modular configuration of the platform also allows rapid electrode replacement and flexible polarity configuration, enabling systematic comparative studies under different experimental conditions [3], [4].

Experimental observations showed that the degradation of the contact surface was concentrated near the center of the contact area. The analyzed regions presented melt pool formation, shallow crater development, material redistribution and surface oxidation, which are typical effects produced by electrical arc exposure [5], [6]. No macroscopic cracking was observed on the tested samples, suggesting that the degradation process was mainly governed by localized melting and re-solidification of the material rather than explosive ejection or brittle fracture [7].

Electro–thermal simulations indicated a strong concentration of the electric field and current density near the arc root region. These results correlate with the experimentally observed erosion zone and confirm the regions where the highest thermal stress occurs on the contact surface [4], [6]. The agreement between simulation results and experimental observations validates both the interpretation of the degradation mechanisms and the functionality of the developed test bench [8].

Overall, the developed platform provides a reliable and electrically insulated system for the study of arc erosion, polarity effects and electro–thermal phenomena in low-voltage switching devices [1], [3], [5].

6. REFERENCES

1. Stasac, C.O., Hoble, D.A., Costea, T., Moldovan, L., *Analysis of Contact Resistance Variation in Electric Devices Under Electric Charge*, 15th International Conference on Engineering of Modern Electric Systems (EMES), pp. 225–228, (2019).
2. Liu, L., Wang, X., Li, H., Fei, Y., Zhang, H., Xue, Z., *Correlation of Contact Bounce and Arc Behavior for Ag-Based Contact Materials under Resistive and Inductive Load*, Wear, Vol. 586, 206447, (2026).
3. Hoble, D.A., Stasac, C.O., *Study on the Influence of Vibrations on Electrical Contact Resistance*, International Conference on Engineering of Modern Electric Systems (EMES), (2015).
4. Kadechkar, A., Riba, J.R., Rojas-Dueñas, G., Martinez, J.A., Moreno-Eguilaz, M., *Experimental Study of the Effect of Aeolian Vibrations on the Contact Resistance of Substation Connectors*, 2020 IEEE International Conference on Industrial Technology (ICIT), 26–28 February, (2020).
5. Hoble, D.A., Stasac, C.O., *Study of the Thermic Effects in the Electric Contacts Subject to the Vibratory Movements*, 14th International Conference on Engineering of Modern Electric Systems (EMES), (2017).
6. Niu, C., Ding, J., Wu, Y., Yang, F., Dong, D., Fan, X., Rong, M., *Simulation and Experimental Analysis of Arc Motion Characteristics in Air Circuit Breaker*, Plasma Science and Technology, Vol. 18, No. 3, pp. 241–246, (2016).
7. Kolimas, Ł., *Analysis of the Breakdown and Electrical Arc in the Process of Switching On*, GSTF Journal of Engineering Technology, Vol. 2, No. 10, (2014).
8. Stasac, C.O., Hoble, D.A., *Comparative Analysis of the Influence of Striction Resistance and Disturbing Pellicles on the Contact Resistance*, 16th International Conference on Engineering of Modern Electric Systems (EMES), 10–11 June, (2021).
9. Lin, J., Liu, H., Lu, S., Yang, Z., Li, C., Zou, K., *Experimental Study of Ignition Process Caused by Poor Electrical Contact of Connector*, Process Safety and Environmental Protection, Vol. 189, pp. 1517–1526, (2024).